J Mater Sci (2006) 41:6889–6894
DOI 10.1007/s10853-006-0935-5

Controllable synthesis and magnetic properties of Fe–Co alloy nanoparticles attached on carbon nanotubes

Hua-Qiang Wu · Pin-Shi Yuan · Hong-Yan Xu · Dong-Mei Xu · Bao-You Geng · Xian-Wen Wei

Received: 10 August 2005 / Accepted: 20 December 2005 / Published online: 5 October 2006

Abstract Fe–Co alloy nanoparticles with different size were attached on the carbon nanotubes through adjusting the ratio of the metal to carbon in the mixed solution of nitrate with Fe:Co = 1:1 (molar ratio) via wet chemistry. X-ray powder diffraction (XRD), transmission electron microscopy (TEM), high-resolution transmission electron microscopy (HRTEM) and energy-dispersive X-ray spectrometry (EDX) indicated that the Fe–Co alloy nanoparticles attached on the surface of carbon nanotubes has body-centered cubic (bcc) structure, with sizes in the range of 13–25 nm and in the shape of spheroids. Magnetization measurements indicated that both the coercivities and the saturation magnetizations altered with size changes of the Fe–Co alloy nanoparticles. The saturation magnetization decreases with decreasing the Fe–Co alloy nanoparticles' sizes. A decrease in coercivity with increasing Fe–Co size together with a local maximum coercivity at size of ca. 15 nm is visible. A linear relationship between the inverse particle diameter and the coercivity was found for larger particles. These demonstrated that the chemical method here is promising for fabricating Fe–Co alloy nanoparticles coated on carbon nanotubes for magnetic storage applications.

H.-Q. Wu (✉) · P.-S. Yuan · H.-Y. Xu · D.-M. Xu · B.-Y. Geng · X.-W. Wei
College of Chemistry and Materials Science, Anhui Key Laboratory of Functional Molecular Solids, Anhui Normal University, Wuhu 241000, P. R. China
e-mail: wuhuaq@yahoo.com.cn

X.-W. Wei
e-mail: xwwei@mail.ahnu.edu.cn

Introduction

Carbon nanotubes are known for their unique structure and mechanical [1], chemical [2] and electronic [3] properties, and their potential applications. The study of metal-coated carbon nanotubes is now becoming a promising and challenging area of research owing to their unique applications such as nanoelectronic devices [4], support media in heterogeneous catalysis [5, 6], fuel cells [7, 8], and magnetic recording [9]. As is well known, there have been various approaches to attach metal nanoparticles on the surface of carbon nanotubes, such as electrochemical deposition [10], electroless plating [11], chemical evaporation deposition [12], solid-state reaction [13], reduction in supercritical carbon dioxide [14] and chemical decoration [15]. As for bimetallic systems or alloys attached on carbon nanotubes, there are few reports. Only Pt–Ru nanoparticles supported on carbon nanotubes by the carbonization of polypyrrole on alumina membrane [16], Co–B coated on carbon nanotubes by chemical reduction method [9] and cluster-derived bimetallic nanoparticles deposited onto carbon nanotubes [17], have been reported. Since Fe–Co alloys are used in the electronic bearings and power generators of aircraft engines [18, 19], and in computer read/write heads and microelectromechanical systems [20] as magnetic recording write head and microactutors [21], we are interested in the preparation of Fe–Co alloy nanoparticles attached on carbon nanotubes.

In this work, the body-centered cubic phase Fe–Co alloy nanoparticles with diameter in the range from 13 nm to 25 nm were attached on the carbon nanotubes in a controllable way by wet chemistry. The

structure, morphology and magnetic properties of Fe–Co alloy nanoparticles are presented.

Experimental

The multi-walled carbon nanotubes (MWNTs), prepared by the thermal catalytic decomposition of hydrocarbons, had an inner diameter in the range of 3–10 nm and an outer diameter in the range of 20–50 nm (with lengths of up to a few microns), which were checked by HRTEM [22]. The procedure employed by us for preparing Fe–Co alloy nanoparticles attached on carbon nanotubes is as follows. In a typical synthesis, the MWNTs (200 mg) were first treated with boiling HNO_3 (68%, 50 cm^3) for 5 h, then washed with triply distilled water. The acid-treated carbon nanotubes were stirred with 50 cm^3 of mixed $Fe(NO_3)_3$ and $Co(NO_3)_2$ solution (Fe:Co = 1:1 atom ratio) for 2 h at room temperature, then strongly stirred at 100 °C until the solvent was evaporated completely. The samples were calcined at 300 °C for 4 h under an argon atmosphere and then reduced under H_2 for 6 h at 400 °C, then cooled naturally to room temperature. By varying the molar ratios of metal (atom ratio Fe:Co = 1:1) to carbon with 2%, 3%, 5%, 7%, and 10%, respectively, the five samples were synthesized.

X-ray power diffraction (XRD) was carried out on an XRD-6000 (Japan) X-ray diffractometer with a Cu–Kα radiation (λ = 0.154060 nm) at a scanning rate of 0.05°s^{-1} in the 2θ range from 10° to 90°. Transmission electron microscopy (TEM) micrographs were taken using a Hitachi H–800 transmission electron microscope, with an accelerating voltage of 200 kV. High-resolution transmission electron microscopy (HRTEM) and energy-dispersive X-ray (EDX) spectrometry were performed using JEM 2010 F field emission microscope. Magnetization was measured at room temperature by a vibrating sample magnetometer (VSM, Japan BHV–55).

Results and discussion

XRD characterization

Figure 1 displays the XRD patterns of the five as-synthesized samples, which show the presence of characteristic reflections of the body centered cubic (bcc) phase of the Fe–Co alloy nanoparticles. The peaks at 2θ values of 44.81°, 65.29° and 82.64° correspond to the crystal planes of (110), (200) and

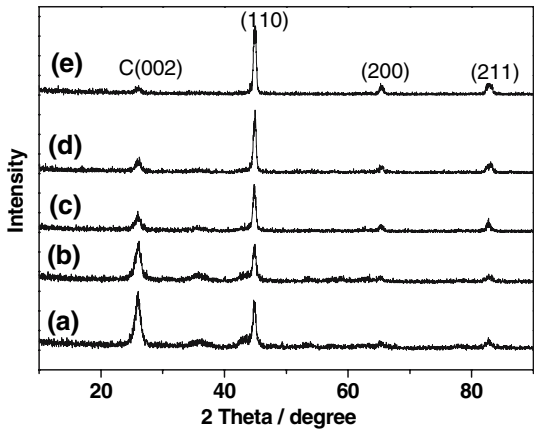

Fig. 1 XRD patterns of the samples with different molar ratio (**a**) 2%, (**b**) 3%, (**c**) 5%, (**d**) 7%, (**e**) 10% of metals (Fe:Co = 1:1) to carbon, respectively

(211) of the crystalline Fe–Co alloy (JCPDS 49–1567), respectively. It is obvious that the peak at 2θ value of 25.97° is caused by the carbon nanotubes. It was found from Fig. 1a–e that the relative intensity ratio of (110) peak of Fe–Co alloy to (002) peak of carbon nanotubes is increased obviously with increasing the molar ratio of Fe–Co alloy to the carbon nanotubes. The cell constant of Fe–Co is calculated to be a = 0.2857 nm, which is in agreement with the reported values of a = 0.2855 nm [23] for particles of the same composition. The average sizes of the Fe–Co alloy nanoparticles, calculated using the Debye-Scherrer formula based on the full width at half-maximum (FWHM) of the (110) diffraction peaks, were 11.9 nm, 12.6 nm, 15.0 nm, 15.3 nm, 15.5 nm at molar ratio of 2%, 3%, 5%, 7%, 10% of metal to carbon, respectively. The results indicated that the alloy sizes are increased from 11.9 nm to 15.5 nm with the increasing of relative ratios of metals to carbon from 2% to 10%.

TEM and HRTEM images

Figure 2 shows the TEM images of Fe–Co alloy nanoparticles attached on the surface of carbon nanotubes at different ratios of metal to carbon. It can be seen that the Fe–Co alloy nanoparticles are in the shape of spheroid on the outer surface of carbon nanotubes. On the whole, the quantity of the Fe–Co alloy nanoparticles attached on carbon nanotubes is increased with increasing the ratio of the metal to carbon and the Fe–Co alloy nanoparticles have a few agglomerations at ratio of 10%. The distributions of the Fe–Co alloy nanoparticle size measured from the TEM images were shown in the Fig. 3. The average values of the alloy nanoparticles sizes measured from

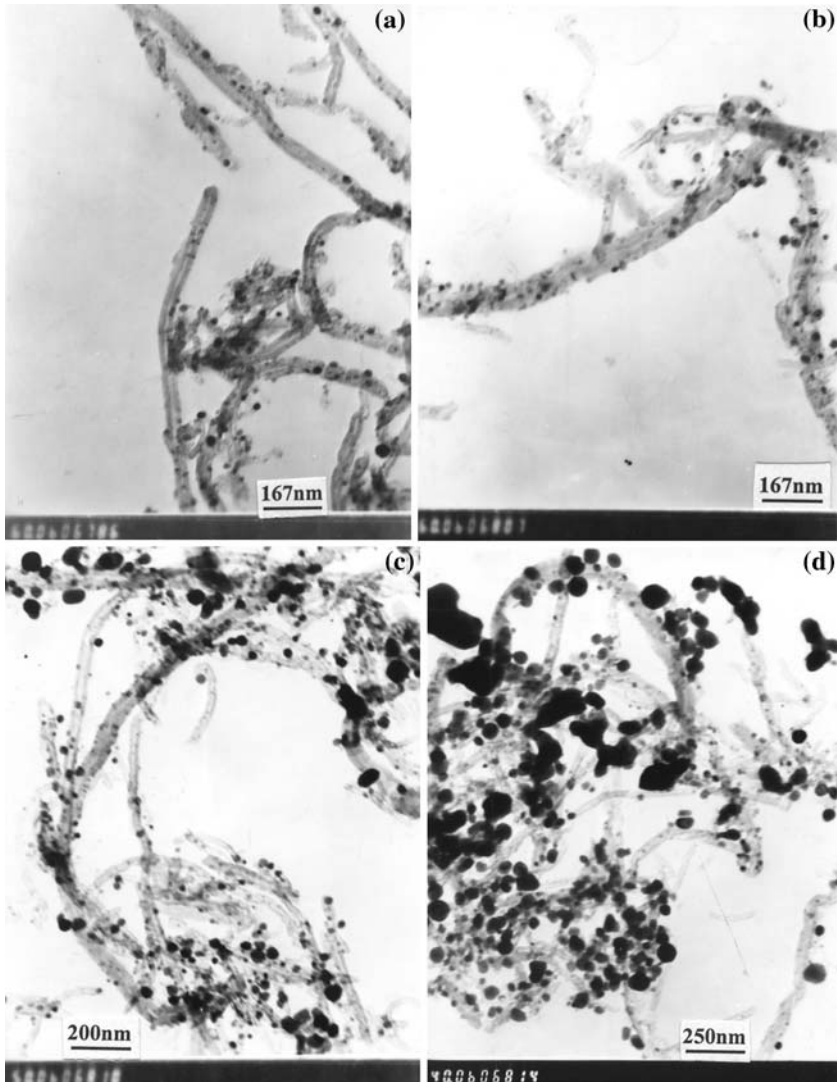

Fig. 2 TEM images of the Fe–Co alloy nanoparticles with different metal (Fe:Co = 1:1) to carbon molar ratio of (**a**) 2%, (**b**) 3%, (**c**) 7%, (**d**) 10%, respectively

the TEM images were 13.3 nm, 15.2 nm, 18.3 nm, 21.4 nm, 24.5 nm at metal to carbon ratios of 2%, 3%, 5%, 7%, 10%, respectively. With the ratio of metal to carbon increases, the size of nanoparticles increases. This trend is consistent with the trend of the size's changes of that were calculated from Debye-Scherrer formula. But the alloy size measured from the TEM image is slight larger than that calculated from Debye-Scherrer formula under the same molar ratio of metal to carbon. Possible reasons for this discrepancy include the contributions of microstrains to line broadening [24], and the differences between volume-weighted averaging in XRD and number-weighted averaging for TEM. These results indicated that the size of Fe–Co alloy nanoparticles can be controlled by adjusting the ratio of metal to carbon nanotubes in the mixed solution of nitrates with atom ratio Fe:Co = 1:1, and that carbon nanotubes are efficient templates in the synthesis of nanoscale metal alloy nanoparticles.

Close examination of the Fe–Co alloy nanoparticles attached on the carbon nanotubes (Fig. 4a) showed lattice fringes with an observed fringe separation of 2.06 Å, consisted with the interlayer separation of the (110) crystal plane of Fe–Co alloy. It is interesting to note that the (110) Fe–Co alloy plane is always parallel to the graphite layer (002) of the tube. The selected area electron diffraction (SAED) pattern shows the presence of diffraction rings (the smallest diffraction ring is belong to carbon nanotubes) due to the (110), (200) and (211) planes, as shown in Fig. 4b, signifying the crystalline nature of Fe–Co (JCPDS 49-1567).

The chemical composition of the alloy nanoparticles attached on carbon nanotubes was analyzed using the energy-dispersive X-ray spectrometer attached to the high-resolution electron microscope. The EDX spectrum (Fig. 5) of an individual nanoparticles shows the presence of iron, cobalt, carbon and copper. It is

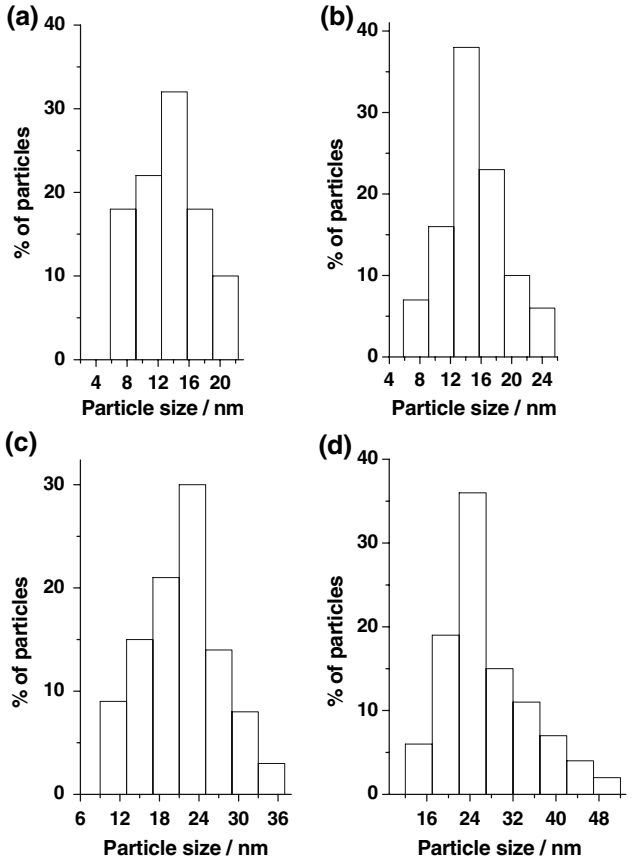

Fig. 3 Fe–Co alloy crystallite average sizes distributions measured from the TEM images at different metal to carbon ratio of (**a**) 2%, (**b**) 3%, (**c**) 7%, (**d**) 10%, respectively

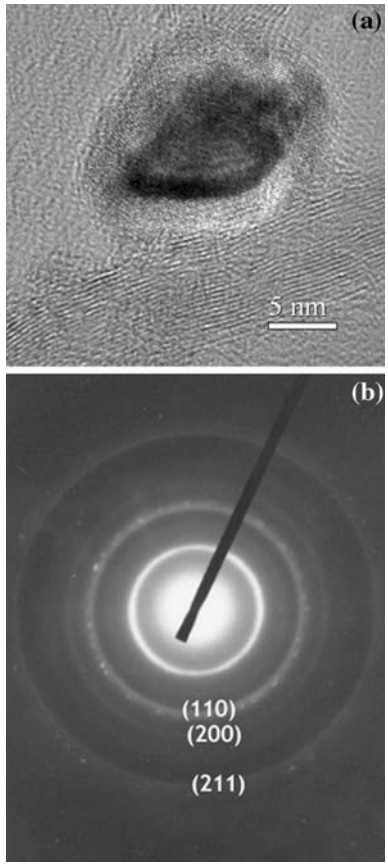

Fig. 4 (**a**) HRTEM image and (**b**) selected area electron diffraction pattern of Fe–Co alloy nanoparticles attached on carbon nanotubes

obvious that the copper peak is caused by the copper grid used to clamp the nanoparticles. The carbon comes from the carbon nanotubes. The tiny amount of oxygen may be originated in the oxide film because nanoparticles of the sizes observed here will inevitably oxidize under ambient conditions. FeCo nanoparticles can be suspended in dry toluene and slightly oxidized to make them air stable. EDX quantitative microanalysis indicates a composition of Fe (52.5%) and Co (47.5%). It was noted that the composition of Fe–Co alloy attached on the surface of carbon nanotubes formed from their mixed nitrate solution was close to the original composition of nitrates.

A possible mechanism of formation of the nanoparticles may be as follow. During the acid-treated process, the carbon nanotubes were activated by nitric acid and various functional groups such as –COOH, –OH, and –C=O were created on the surface of carbon nanotubes, which can act as nucleation sites for metal cluster [15]. On the other hand, the multi-walled carbon nanotubes contain defects on the outer surface [25]. Nitrate salts combined with the carbon nanotubes through active center and the defect sites on the outer surface of carbon nanotubes. In the course of heat-treatment, the decomposition of the oxide precursor (nitrate salts) in the hot zone of the nanotubes gives rise to the metal oxide crystals in situ [26]. Then, the metal oxides would be reduced by hydrogen to the native metals [27], thus forming the crystalline alloy nanoparticles.

Magnetic properties

Magnetic properties of samples were investigated at room temperature using a vibrating sample magnetometer with an applied field $-10\ \text{kOe} \le H \le 10\ \text{kOe}$. Figure 6 shows the magnetic hysteresis loops for samples with metal to carbon ratios of 2%, 3%, 5%, 7% and 10%, respectively, which are the typical loops of soft magnet. Figure 7a shows a decrease of the saturation magnetizations with decreasing nanoparticles size. Such behavior has already been observed with ferrite nanoparticles [28, 29]. This may be due to an increase in the disorder of the orientation of magnetic

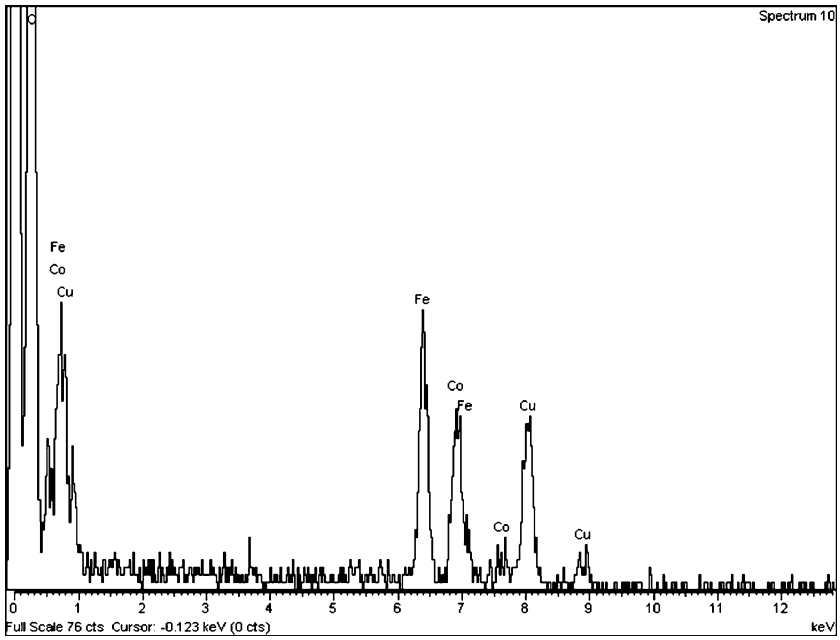

Fig. 5 EDX spectrum of the Fe–Co alloy on carbon nanotubes with metal to carbon ratio of 3%

moments in the various sites when the ratio surface/volume increases [30, 31].

The particle size dependence of the coercivity is shown in Fig. 7b, a decrease in coercivity with increasing particle size together with a local maximum at about 15 nm is visible, which are in agreement with the previous report [32]. For 13 nm < D < 15 nm, the coercivity increases with increasing particle size and exhibits the usual particle size dependence on coercivity, which overcompensates in this particle size range the otherwise predominant strain influence [32]. For larger nanoparticle sizes, the coercivity has a decrease with increasing particle size. The size dependence of the coercivity is connected with the domain structure and the particle size. Favorably oriented domains grow at the expense of those not aligned with the applied field. As domain walls move through a sample, they can become pinned at particle boundaries, and additional energy is needed for them to continue moving [33]. Therefore, reducing the particle size creates more pinning sites and increases the coercivity. The coercivity for the particles with size of more than 15 nm can be fitted by a function proportional to $1/D$ (see Fig. 8) as is predicted for magnetization processes determined by domain wall pinning, i.e. with increasing particle size the magnetization process changes from random anisotropy to the domain structure.

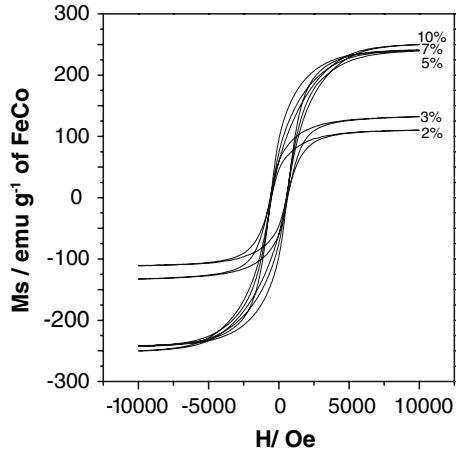

Fig. 6 Hysteresis loop of the samples measured at room temperature

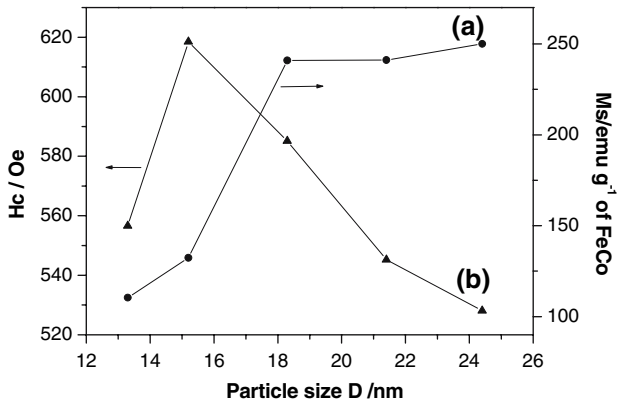

Fig. 7 (**a**) Saturation magnetization as a function of the average particle size D (nm); (**b**) The variation of the coercivity Hc with the average particle size of Fe–Co alloy nanoparticles

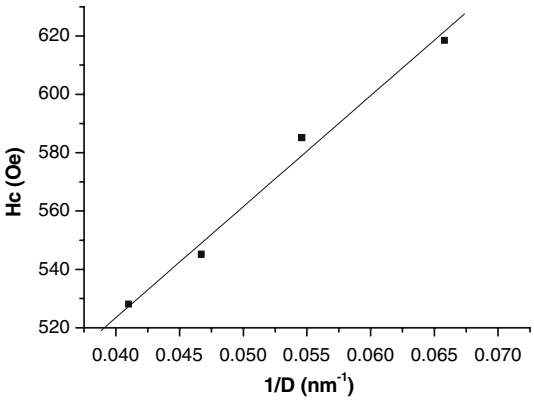

Fig. 8 The coercivity versus inverse particle diameter $1/D$ for larger particles

Conclusions

The body-centered cubic phase Fe–Co alloy nanoparticles with diameter in the range from 13 nm to 25 nm were successfully attached on the surface of carbon nanotubes by wet chemistry. The alloy nanoparticle sizes can be controlled through adjusting the metals/CNT molar ratio in the mixed solution of nitrates with Fe:Co = 1:1(atom ratio). Magnetic measurements show that Fe–Co alloy nanoparticles attached on carbon nanotubes have good soft magnetic in nature, both the coercivities and the saturation magnetizations altered with changing the size of the Fe–Co alloy nanoparticles. The saturation magnetization decreases with decreasing Fe–Co nanoparticle size. The coercivity decreases with increasing Fe–Co alloy nanoparticle size, and a local coercivity maximum at about 15 nm appeared. A linear relationship between the inverse grain diameter and the coercivity was found for larger particles. The above results evidently demonstrate that the chemical method employed here is promising for fabricating Fe–Co alloy nanoparticles coated on carbon nanotubes for magnetic storage applications.

Acknowledgements We thank Anhui Provincial Excellent Young Scholars Foundation (No. 04046065), the Education Department (Nos. 2003KJ140, 2001KJ115ZD) of Anhui Province, the State Education Ministry (EYTP, SRF for ROCS) and National Natural Science Foundation (Nos. 20271002, 20490210) of P. R. China for financial support.

References

1. Poncharal P, Wang ZL, Ugarte D, Heer WAD (1999) Science 283:1513
2. Chen J, Hamon MA, Hu H, Chen YS, Rao AM, Eklund PC, Haddon RC (1998) Science 282:95
3. Frank S, Poncharal P, Wang ZL, Heer WAD (1998) Science 280:1744
4. Dai HJ, Wong EW, Lieber CM (1996) Science 272:523
5. Cop B, Planeixb JM, Brotons V (1998) Appl Catal A Gen 173:175
6. Liu ZJ, Xu ZD, Yuan ZY, Lu DY, Chen WX, Zhou WZ (2001) Catal Lett 72(3–4):203
7. Steigerwalt ES, Deluga GA, Lukehart CM (2002) J Phys Chem B 106:760
8. Che GL, Lakshmi BB, Martin CR, Fisher ER (1999) Langmuir 15(3):50
9. Liu ZJ, Xu ZD, Yuan ZY, Chen WX, Zhou WZ, Peng LM (2003) Mater Lett 57:1339
10. Xu Q, Zhang L, Zhu J (2003) J Phys Chem B 107:8294
11. Ang LM, Hor TSA, Xu GQ, Tung CH, Zhao SP, Wang JLS (2000) Carbon 38:363
12. Kong J, Chapline MG, Dai HJ (2001) Adv Mater 13(18):1384
13. Xue B, Chen P, Hong Q, Lin JY, Tan KL (2001) J Mater Chem 11:2378
14. Ye XR, Lin YH and Wai CM (2003) Chem Commun 642
15. Satishkumar BC, Vogl EM, Govindaraj A, Rao CNR (1996) J Appl D:Appl Phys 29:3173
16. Rajesh B, Ravindranathan TK, Bonard JM, Viswanathan B (2000) J Mater Chem 10(8):1757
17. Hermans S, Sloan J, Shephard DS, Johnson BFG, GreenMLH (2002) Chem Commun 276
18. Shang CH, Weiths TP, Cammarata RC, JI Y, Chien CL (2000) J Appl Phys 87(9):6508
19. Gautard D, Couderchon G, Coutu L (1996) J Magn Magn Mater 160:359
20. Kim D, Park DY, Yoo BY, Sumodjo PTA, Myung NV (2003) Electrochim Acta 48:819
21. Shao I, Vereecken PM, Chien CL, Cammarata RC, Searson PC (2003) J Electrochem Soc 150(3):C184
22. Liu BC, Tang SH, Liang Q, Gao LZ, Zhang BL, Qu MZ, Yu ZL (2001) Chin J Chem 19(10):983
23. Joint Committee on Powder Diffraction Standards, Diffraction Data File, No:49 –1567 JCPDS International Center for Diffraction Data, Pennsyivania, 1991
24. Fenineche NE, Hamzaoui R, El Kedim O (2003) Mater Lett 57:4165
25. Arai S, Endo M, Aneko NK (2004) Carbon 42:641
26. Satishkumar BC, Govindaraj A, Nath M, Rao CNR (2000) J Mater Chem 10(9):2115
27. Tsang SC, Chen YK, Harris PJF, Green MLH (1994) Nature 372:159
28. Coey JMD (1971) Phys Rev Lett 27:1140
29. Morrish AH, Haneda K (1981) J Appl Phys 52:2496
30. Hochepied JF, Bonville P, Pileni MP (2000) J Phys Chem B 104:905
31. Berkowitz AE, Kodama RH, Makhlouf SA, Parker FT, Spada FE, Mcniff EJ Jr, Foner S (1999) J Magn Magn Mater 196–197:591
32. Kuhrt C, Schultz L (1993) J Appl Phys 73(10):588
33. Majetich SA, Scott JH, Kirkpatrick EM, Chowdary K, Gallagher K, Mchenry ME (1997) Nanostruct Mater 9:291